**Advanced Technologies for Hypersonic Propulsive, Energetic and Reusable Platforms Technical Conference and Exposition**
**30th of July of 2021**

# DETONATION WAVE FREQUENCY ANALYSIS THROUGH DYNAMIC MODE DECOMPOSITION

**Kian Garcia**
University of Central Florida
Orlando, FL

**Dr. Kareem Ahmed**
University of Central Florida
Orlando, FL

## ABSTRACT

*With deflagration-based combustion being shown to be inefficient compared to detonation-based combustion, rotating detonation engines (RDEs) are one example which use detonation-based combustion. RDEs, when powered, produce detonation waves that rotate around the annulus of the RDE (hence the name). These detonation waves rotate at a certain frequency and this paper will show how to find these frequencies with dynamic mode decomposition (DMD). DMD is a method to identify structures with space and time data from data that has been used in other fluid mechanics before. DMD takes two matrices of identical dimensions and finds a linear approximation between the two matrices by taking the singular value decomposition of one of the matrices into three more matrices (**U**, **Σ**, and **V**) with highly specific characteristics, truncating said matrices to save energy, and finding the linear approximation from these new matrices. The frequency analysis can be done with the **V** matrix and there are two frequency analyses done, Fast Fourier Transform and Welch's Method. This is all done through MATLAB with tiff images of the detonation waves taken from a high-speed camera.*

Keywords: {example}, {example}, {…}

## NOMENCLATURE

| | |
|---|---|
| RDE | Rotating Detonation Engine |
| PDE | Pulse Detonation Engine |
| DMD | Dynamic Mode Decomposition |
| POD | Proper Orthogonal Decomposition |
| SVD | Singular Value Decomposition |
| PFV | Photron Fastcam Viewer |
| $\mathbf{X}$ | Matrix of Spacial and Temporal Data |
| $\mathbf{X'}$ | Matrix with same dimensions as $\mathbf{X}$, except shifted by one column |
| m | Number of columns in matrices that represent temporal data |
| n | Number of rows in matrices that represent spacial data |
| $\mathbf{A}$ | Linear Approximator of matrices $\mathbf{X}$ and $\mathbf{X'}$ |
| $\mathbf{U}$ | Unitary and orthonormal matrix |
| $\mathbf{V}$ | Unitary and orthonormal matrix |
| $\mathbf{\Sigma}$ | Matrix with non-zero values on the diagonals and zeros off the diagonals |
| $\sigma_k$ | $k^{th}$ element of the diagonals of the $\mathbf{\Sigma}$ matrix |
| r | ranked value that reduces matrix dimensions to save energy when doing DMD analysis |
| $\tilde{\mathbf{X}}$ | Ranked $\mathbf{X}$ matrix |
| $\tilde{\mathbf{U}}$ | Ranked $\mathbf{U}$ matrix |
| $\tilde{\mathbf{V}}$ | Ranked $\mathbf{V}$ matrix |
| $\tilde{\mathbf{\Sigma}}$ | Ranked $\mathbf{\Sigma}$ matrix |
| $\mathbf{\Lambda}$ | Eigenvalues of $\mathbf{A}$ |
| $\mathbf{W}$ | Eigenvectors of $\tilde{\mathbf{A}}$ |
| $\mathbf{\Phi}$ | DMD Modes |
| FFT | Fast Fourier Transform |
| FT | Fourier Transform |
| DFT | Discrete Fourier Transform |

## 1. INTRODUCTION

Detonation-based combustion has become a popular source of power due to its rapid energy release [1] and its increase in efficiency [2] compared to deflagration-based combustion. Deflagration-based combustion has been the standard form of energy conversion for jet and liquid rocket propulsion [1] but the tradeoff, compared to detonation-based propulsion, is the cyclic nature of deflagration that uses a constant pressure approach (starting at the constant pressure line at point 2 at Figure 3) at the trade-off of consumption of energy whereas detonation forces a pressure gain increases work and system efficiencies [2]. Detonation is a shock wave sustained by energy from combustion characterized by the ignition (by a flame) of a combustible mixture at a closed end of a tube with an open opposite end [3]. RDEs use this ignition to have a continuous detonation and a higher impulse per unit area compared to PDEs which detonate once every pulse with a lower impulse per unit area [1]. Figure 1 shows a simplified schematic of an RDE with the reactants being injected into the combustor (Figure 2 [1]).

 

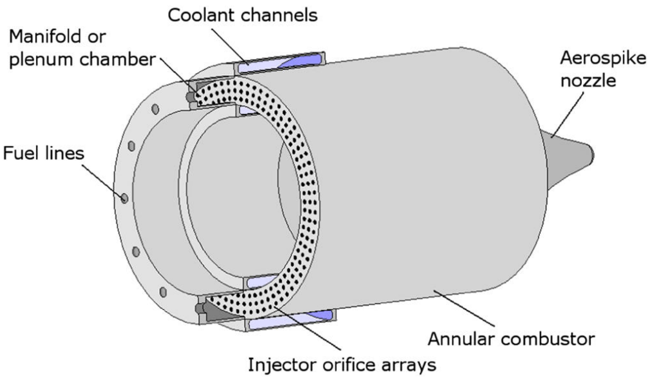

**Figure 1: Schematic of conceptual RDE [1]**

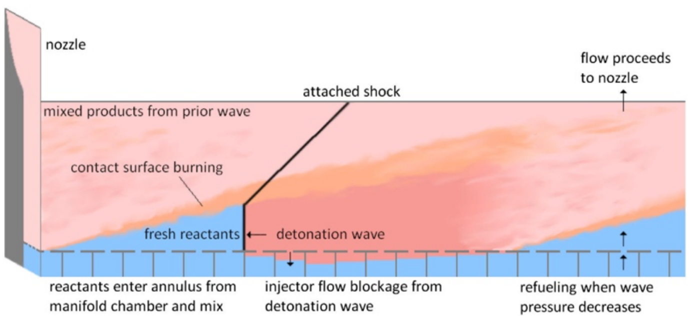

**Figure 2: Rotating wave structure sketch [1]**

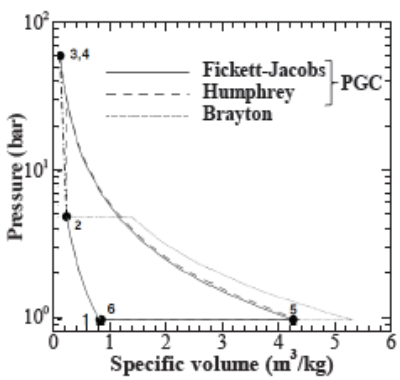

**Figure 3: Pressure-specific volume comparison of Idealized Thermodynamic Cycles [2]**

The RDE cycle is sustained through continuously mixed fuel and oxidizer flows [1], creating detonation waves that circle around the annulus (Figure 1). Mechanics that form these waves include turbulent flows, good mixing of fuels and oxidizers, and time delay between fuel initiation and ignition [1]. Characteristics of these detonation waves are frequency, speed, and wave number [2]. Measuring the characteristics of detonation waves required high-speed cameras that took high-speed images and analyzed the characteristics frame by frame, calculating these characteristics through the following means: image correction, annulus location determination, cartesian mesh integration, and frequency domain analysis [4].

DMD is a way to identify spatio-temporal coherent structures from high-dimensional data in fluid mechanics [6]. It utilizes POD and SVD [6]. The main difference between DMD that DMD uses both spacial and temporal data whereas POD and SVD only look at spatial data by providing a modal decomposition of modes consisting of spatially correlated structures with similar time related linear behavior [6]. One study has used DMD with rotating detonation waves of a rotating detonation combustor, looking at the wave frequency and wave modes [7]. Other applications of DMD regarding fluid mechanics include mixing, acoustics, and wake flows [6].

## 2. MATERIALS AND METHODS

To analyze the detonation waves via any method, they had to be set in the form of tiff files that represented each frame. The detonation waves were recorded with a high-speed camera (specify which camera was used later) that recorded at sampling rates. To get the tiff files needed for the analysis, the frames of the video needed to be extracted via PFV.

PFV is a computer software that controls the Photron high-speed camera series. This allows users to look at frames from videos produced by these cameras. Properties that were used for this were the frame extraction and the frames per second. Figure 4 displays the PFV interface. The main objective was to collect the frequency through DMD via MATLAB.

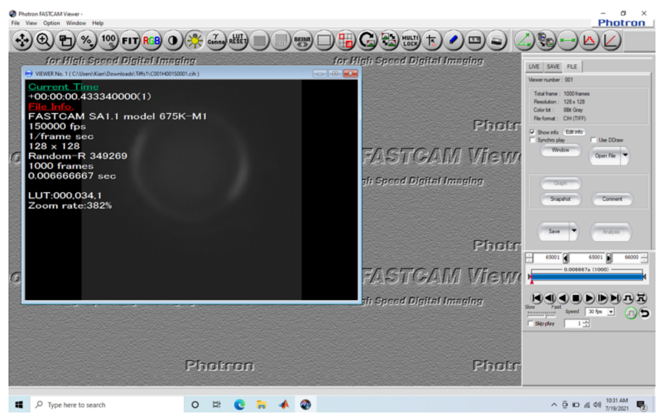

**Figure 4: PFV Interface**

Figure 4 also shows an example of a tiff of detonation waves that would be analyzed for its frequency rate.

### 2.1 An Overview of DMD

The way the DMD works is that collected pairs of snapshots of a system's state evolving in time are arranged into two data matrices **X** and **X′** the assumption that there are equal time intervals between each snapshot [6].

$$\mathbf{X} = \begin{bmatrix} | & | & & | \\ \mathbf{x}_1 & \mathbf{x}_2 & \cdots & \mathbf{x}_m \\ | & | & & | \end{bmatrix}$$

$$\mathbf{X}' = \begin{bmatrix} | & | & & | \\ \mathbf{x}_2 & \mathbf{x}_3 & \cdots & \mathbf{x}_{m+1} \\ | & | & & | \end{bmatrix}$$

**Figure 5: Relation Between X and X′ Matrices [6]**

Figure 5 demonstrates the connection between the two matrices. Because of this connection, we can assume that matrix $\mathbf{X'}$ has the same element composition as the matrix $\mathbf{X}$. The algorithm tries to form a matrix A using both $\mathbf{X}$ and $\mathbf{X'}$ matrices to make the linear approximation $\mathbf{X'} \approx \mathbf{AX}$. The algorithm works by taking the $\mathbf{X}$ matrix and computes its SVD: $\mathbf{X} \approx \mathbf{U\Sigma V^*}$ in which $\mathbf{U} \in \mathbb{C}^{n\times n}$, $\mathbf{\Sigma} \in \mathbb{R}^{n\times m}$, and $\mathbf{V} \in \mathbb{C}^{m\times m}$. Matrices $\mathbf{U}$ and $\mathbf{V}$ are unitary and orthogonal while matrix $\mathbf{\Sigma}$ is a matrix with non-zero values on the diagonal with zeros off the diagonal. It is worth noting that these matrices have dominant patterns that can explain the data along with other values that have little value to the data. To eliminate the less relevant data, the three matrices are given rank-approximations, denoted as r. truncate the matrices $\mathbf{U}$, $\mathbf{\Sigma}$, and $\mathbf{V}$ to $\tilde{\mathbf{U}}$, $\tilde{\mathbf{\Sigma}}$, and $\tilde{\mathbf{V}}$, to which $\tilde{\mathbf{U}} \in \mathbb{C}^{n\times r}$, $\tilde{\mathbf{\Sigma}} \in \mathbb{C}^{r\times r}$, and $\tilde{\mathbf{V}} \in \mathbb{C}^{m\times r}$ [6] (Figure 6).

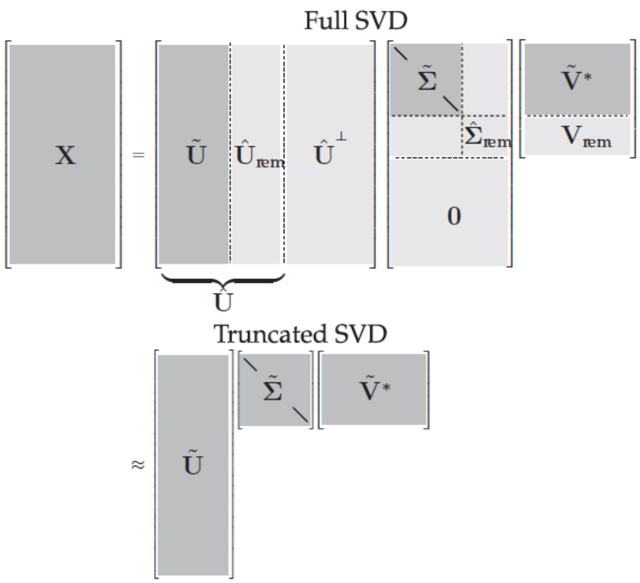


**Figure 6: Full SVD and Truncated SVD of Matrix X [6]**

The criterion for the r value is usually determined by a percent variance in energy of the original data, often referred to as a percent truncation [6]. Equation/Definition 9 shows the criterion used for this research by using the singular values found in the diagonals of the $\mathbf{\Sigma}$ matrix (denoted as $\sigma_k$) [6]. This equation takes the sum of $\sigma_k$ values to any element and divides it by the total sum of $\sigma_k$ to the length of m to find the r value that makes the top denominator greater than a specified percentage (in this research, 99.9% or .999 was used). With these three matrices, we can find $\tilde{\mathbf{A}} = \tilde{\mathbf{U}}^*\tilde{\mathbf{X}}'\tilde{\mathbf{V}}\tilde{\mathbf{\Sigma}}^{-1}$ which approximates the full matrix $\mathbf{A}$ (Equation/Definition 13) with r eigenvectors and eigenvalues and makes the linear approximation $\tilde{\mathbf{x}}_{\mathbf{k+1}} = \tilde{\mathbf{A}}\tilde{\mathbf{x}}_{\mathbf{k}}$ [6]. Next, to compute the spectral decomposition of $\tilde{\mathbf{A}}$, one takes the DMD eigenvalues (denoted as $\mathbf{\Lambda}$ [which correspond to the eigenvalues of $\mathbf{A}$]) to find the eigenvectors of $\tilde{\mathbf{A}}$ (denoted as $\mathbf{W}$) with the equation $\tilde{\mathbf{A}}\mathbf{W} = \mathbf{W\Lambda}$ [6]. Finally, the DMD modes (denoted as $\Phi$) are calculated with the matrices $\mathbf{X'}$, $\tilde{\mathbf{V}}$, $\tilde{\mathbf{\Sigma}}$, and $\mathbf{W}$ in the equation $\mathbf{\Phi} = \mathbf{X'}\tilde{\mathbf{V}}\tilde{\mathbf{\Sigma}}^{-1}\mathbf{W}$ [6].

**TABLE 1:** Equations/Definitions

| Equation/ Definition # | Equation/ Definition Name | Equation/Definition |
|---|---|---|
| 1 | Elements of X Matrix | $\mathbf{X} \in \mathbb{C}^{n\times m}$ |
| 2 | Elements of X′ Matrix | $\mathbf{X}' \in \mathbb{C}^{n\times m}$ |
| 3 | Linear Relation between X and X′ Matrices | $\mathbf{X}' \approx \mathbf{AX}$ |
| 4 | SVD of X | $\mathbf{X} \approx \mathbf{U\Sigma V}^*$ |
| 5 | Elements of **U** Matrix | $\mathbf{U} \in \mathbb{C}^{n\times n}$ |
| 6 | Elements of **Σ** Matrix | $\mathbf{\Sigma} \in \mathbb{R}^{n\times m}$ |
| 7 | Elements of **V** Matrix | $\mathbf{V} \in \mathbb{C}^{m\times m}$ |
| 8 | Ranked **X** Decomposition denoted as $\tilde{\mathbf{X}}$ | $\mathbf{X} \approx \mathbf{U\Sigma V}^*$ (ranked SVD) $\tilde{\mathbf{X}} \approx \tilde{\mathbf{U}}\tilde{\mathbf{\Sigma}}\tilde{\mathbf{V}}^*$ |
| 9 | Criterion to find r | $.999 \geq \frac{\sum_{\mathbf{k=1}}^{\mathbf{r}} \sigma_{\mathbf{k}}}{\sum_{\mathbf{k=1}}^{\mathbf{m}} \sigma_{\mathbf{k}}}$ |
| 10 | Elements of $\tilde{\mathbf{U}}$ Matrix | $\tilde{\mathbf{U}} \in \mathbb{C}^{n\times r}$ |
| 11 | Elements of $\tilde{\mathbf{\Sigma}}$ Matrix | $\tilde{\mathbf{\Sigma}} \in \mathbb{C}^{r\times r}$ |
| 12 | Elements of $\tilde{\mathbf{V}}$ Matrix | $\tilde{\mathbf{V}} \in \mathbb{C}^{m\times r}$ |
| 13 | Matrix **A** | $\mathbf{A} = \mathbf{X}'\tilde{\mathbf{V}}\tilde{\mathbf{\Sigma}}^{-1}\tilde{\mathbf{U}}^*$ |
| 14 | Ranked Matrix **A** (denoted as $\tilde{\mathbf{A}}$) | $\tilde{\mathbf{A}} = \tilde{\mathbf{U}}^*\mathbf{X}'\tilde{\mathbf{V}}\tilde{\mathbf{\Sigma}}^{-1}$ |
| 15 | Spectral Decomposition of $\tilde{\mathbf{A}}$ | $\tilde{\mathbf{A}}\mathbf{W} = \mathbf{W\Lambda}$ |
| 16 | DMD Modes | $\mathbf{\Phi} = \mathbf{X}'\tilde{\mathbf{V}}\tilde{\mathbf{\Sigma}}^{-1}\mathbf{W}$ |

### 2.2 DMD Code

The DMD Code consisted of image processing code [8] as well premade code to apply DMD via MATLAB: the DMD algorithm [6], cumulative energy criterion [6], frequency analysis [9], and DMD Mode analysis [10]. Recalling equation 1 and 2 and that DMD takes account of both spacial and temporal data, assume that m columns capture the temporal data and that n rows represents the spacial data. The image processing involves uploading the tiff files from the high-speed camera recordings of the detonation waves onto MATLAB and gathering all the images (which are now matrices) and rearranging them from the image, which is of a rows and b columns to giant columns of size a times b and putting each of these columns next to each other for all the images. This satisfies creating the matrix needed for DMD.

The first thing to start the DMD algorithm is to create the $\mathbf{X}$ and $\mathbf{X'}$ matrices from the matrix created earlier from the tiff image files (denote this matrix as $\mathbf{T}$). The way to utitilze it via MATLAB with this created matrix is to declare the $\mathbf{X}$ matrix as all the columns of matrix $\mathbf{T}$ from the first column to one column to the end and to declare the $\mathbf{X'}$ matrix as the columns of matrix $\mathbf{T}$ from the second column to the end column. From there, one starts by calling the SVD function to extract the matrices $\mathbf{U}$, $\mathbf{\Sigma}$, and $\mathbf{V'}$ from $\mathbf{X}$ (Equation/Definition 4). The cumulative energy criterion to find r is implented directly after this SVD function call since the MATLAB code needs the matrix $\mathbf{\Sigma}$ for it to work (Figure 7).

```
cdS = cumsum(diag(S))./sum(diag(S));  % Cumulative energy
r90 = min(find(cdS>0.90));  % Find r to capture 90% energy
```

**Figure 7: Example Cumulative Energy Code with *S* as Σ [6]**

Next, the matrices $\mathbf{U}$, $\mathbf{\Sigma}$, and $\mathbf{V'}$ have to be truncated so that they have the elements of $\tilde{\mathbf{U}}$, $\tilde{\mathbf{\Sigma}}$, and $\tilde{\mathbf{V}}$ (respectively), each with the elements in Equations/Definitions 9, 10, and 11, respectively. From there, using those ranked matrices, $\tilde{\mathbf{A}}$ can be found based on Equation/Definition 13, the spectral decomposition of A can be found through Equation/Definition 14, and the DMD modes can be found through Equation/Definition 15. Figure 8 shows an example of the MATLAB code to implement these equations.

```
Atilde = Ur'*Xprime*Vr/Sigmar;       % Step 2
[W,Lambda] = eig(Atilde);            % Step 3

Phi = Xprime*(Vr/Sigmar)*W;          % Step 4
```

**Figure 8: Finding Matrix Ã, its Spectral Decomposition, and DMD Modes Using MATLAB Code [6]**

In Figure 7, *Atilde*, *Ur'*, *Xprime*, *Vr*, *Sigmar*, *W*, *Lambda*, and *Phi* each represent $\tilde{\mathbf{A}}$, $\tilde{\mathbf{U}}'$, $\mathbf{X'}$, $\tilde{\mathbf{V}}$, $\tilde{\mathbf{\Sigma}}$, $\mathbf{W}$, $\mathbf{\Lambda}$, and $\mathbf{\Phi}$, respectively from Equations/Definitions 12, 14 and 15 [6].

The frequency analysis takes the DMD and finds the frequency domain through FFT and the pwelch function [9]. FFT in MATLAB requires the use of the fft function [11].

To understand FFT, one should look at DFT. DFT is, as the name implies, the discrete version of FT (which is continuous). Fast Fourier Transform is an algorithm that finds the DFT of a signal. The criteria to evaluate whether to use FT or DFT is based on whether the data is

This function creates the FFT of the signal, which can then be used to find the two-sided amplitude spectrum which can be used to find the one-sided amplitude spectrum (Figure 9).

```
Y = fft(X);
P2 = abs(Y/L);
P1 = P2(1:L/2+1);
P1(2:end-1) = 2*P1(2:end-1);
f = Fs*(0:(L/2))/L;
plot(f,P1)
```

**Figure 9: Example Code for Fast Fourier Transform Analysis [11]**

In Figure 8, *X*, *Y*, *P2*, *L*, *P1*, *Fs*, and *f* represent the signal as a function, the Fourier transform of the signal, the two-sided amplitude spectrum, the one-sided amplitude spectrum, the sample rate, and the frequency domain [11]. Plotting *f* and *P1* gives the single-side amplitude graph. Note that this method will take the FFT of the entire signal window.

The pwelch function in MATLAB utilizes Welch's method of power spectral density estimation. Recall that the previous method takes the FFT of the entire signal window. Welch's method, instead, takes multiple FFT's of segments of the time domain of the signal with overlaps within different segments throughout the entire signal. Figure 10 gives a visual of Welch's method.

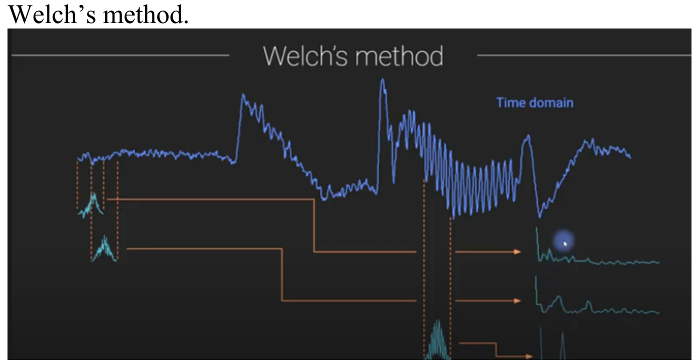


**Figure 10: Welch's Method with Overlapped FFT Segments [13]**

In Figure 10, the FFT is taken in two small segments of the time domain (denoted in purple) with each FFT segment overlapping one another.

This overlap is crucial because the average of the FFTs is taken, creating an estimate of the averages of the Frequency domain of the time domain of the signal. By taking the averages of the FFTs of multiple segments of the time domain of the signal, the result is that the estimate smoothens the frequency domain. Figure 11 demonstrates the frequency domains taken by FFT (denoted as *Full)* vs Welch's method (denoted as *Welch's*) of the signal in Figure 9. Note that, in Figure 9, because Welch's method takes the average FFTs of segments, the overall amplitudes will be much smaller than a full FFT of the entire signal.

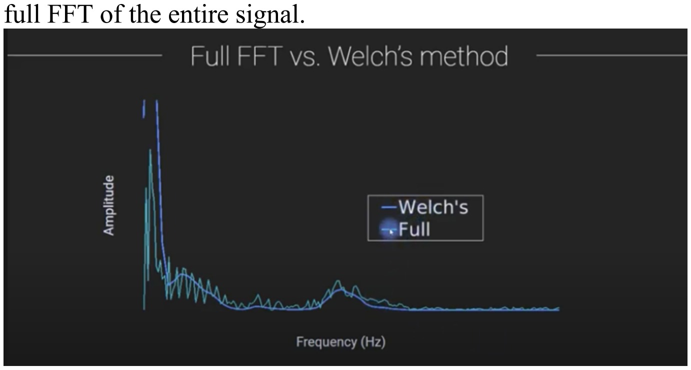


**Figure 11: Frequency Domain using FFT and Welch's Method [13]**

In MATLAB, the pwelch function that is relevant to this testing is of the following form in Figure 12.

```
[pxx,f]= pwelch(x,window,noverlap,nfft,fs)
```

**Figure 12: pwelch Function [13]**

In this function, *pxx*, *f*, *x*, *window*, *noverlap*, *nfft*, and *fs* represent the power spectral density vector, the frequency, the input signal vector, the window (with length of nfft), the number of overlapped samples, the number of points in DFT, and the sample rate in Hz respectively [13]. To reduce the noise further, we utilize the example of DFT averaging [13] with **V** from the SVD as the signal vector, the window as a hanning window of the number of points in DFT, the number of overlapped points as the number of points in DFT divided by two, the number of points in DFT as the number of tiff files divided by two, and the sampling rate in Hz as the frequency rate of the PFV Camera.

The reason that both FFT and Welch's method are used (shown later) is because the nozzle analysis has massive noise that make the frequency domains hard to interpret. If just FFT or Welch's method is used, then, with the amount of noise in the frequency in the nozzles, the one analysis used does not have a similar analysis to compare. Furthermore, the pwelch method with DFT averaging reduces the variance of the noise of the frequency domain by using a hanning window [13] which attempts to get rid of the noise at the ends of the signal as, at those times, there is no DFT averaging [12].

Finally, the DMD Mode Analysis takes the diagonals of the **Λ** matrix and makes a graph that displays the DMD spectrum [10]. When put into a graph, the diagonals of the **Λ** matrix will be plotted around the unit circle [10]. While this is not necessarily relevant to the analysis of the RDE detonation waves nor the analysis of the nozzle, it can be an assurance that the code is working as it should be.

### 2.3 Exhaust Analysis

The exhaust analysis uses the methods mentioned before, but rather than just looking at the detonation waves, this analysis looks at tiff files from different views from the exhaust.

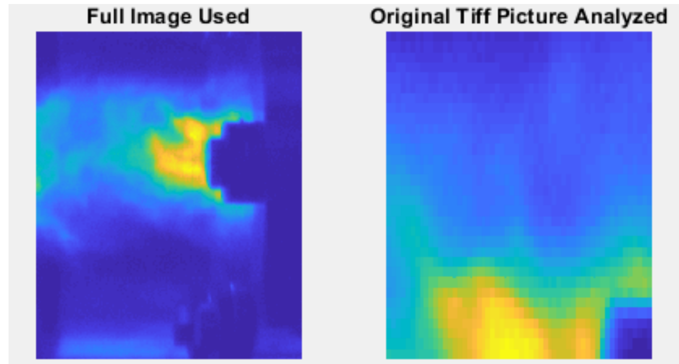


**Figure 13: First Exhaust View for DMD Analysis**

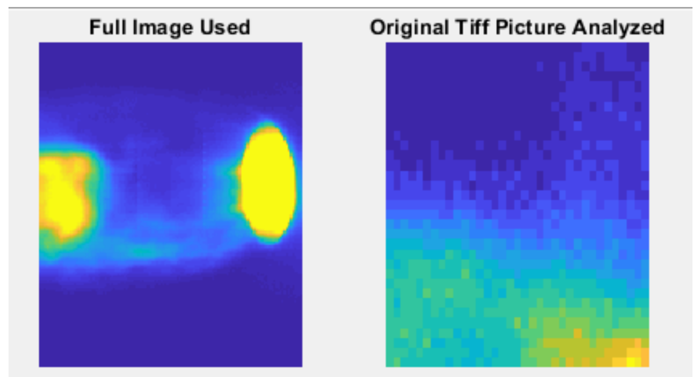


**Figure 14: Second Exhaust View for DMD Analysis**

Furthermore, because this looks at the entire exhaust rather than looking at the just the detonation waves, looking at the entire image for the frequencies would create more noise. Therefore, the best solution to find the frequencies is to crop certain regions of interest that detonation waves are known to propagate. Figures 13 and 14 show different views of the exhaust displayed via MATLAB and the cropped images analyzed.

## 3. RESULTS AND DISCUSSION

 

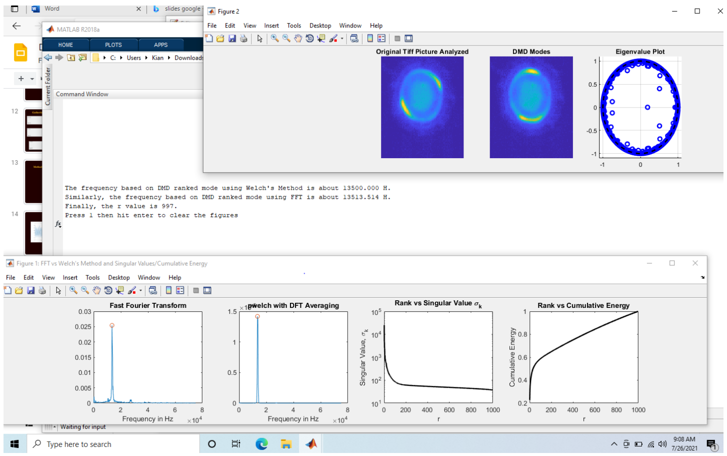


**Figure 15: First Set of Detonation Wave Frequencies Extracted**

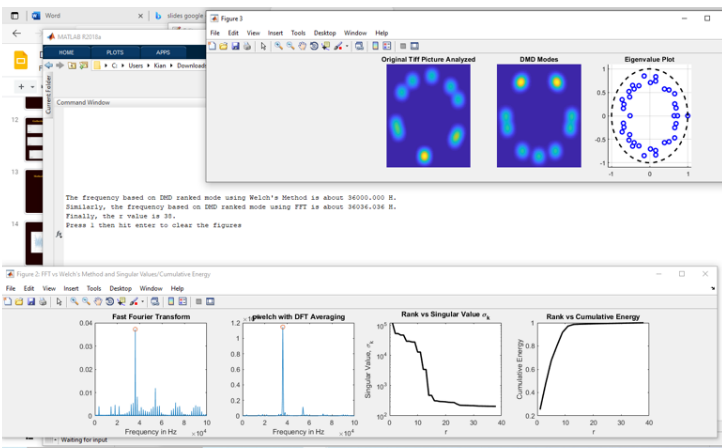


**Figure 16: Second Set of Detonation Wave Frequencies Extracted**

With the first two set tiff files of direct detonation waves, extracting the frequencies is relatively straightforward since there was less "other content" in these tiff files since the main image that is seen in the figures within the figures labeled *Original Tiff Picture Analyzed* and *DMD Modes* are the detonation waves rotating around the annulus of the RDE.

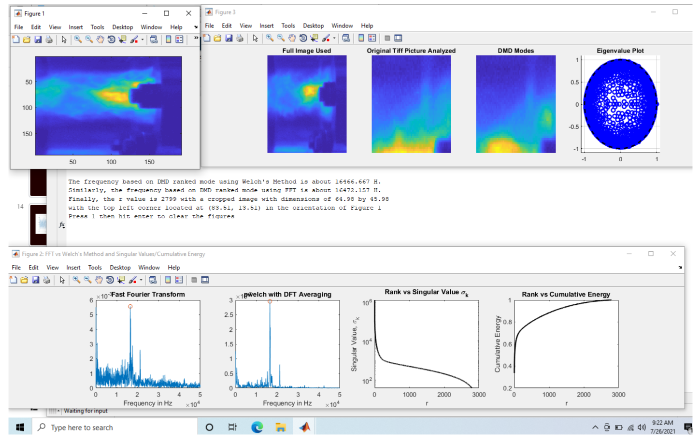


**Figure 17: First Set of Detonation Wave Frequencies Extracted from the Exhaust View**

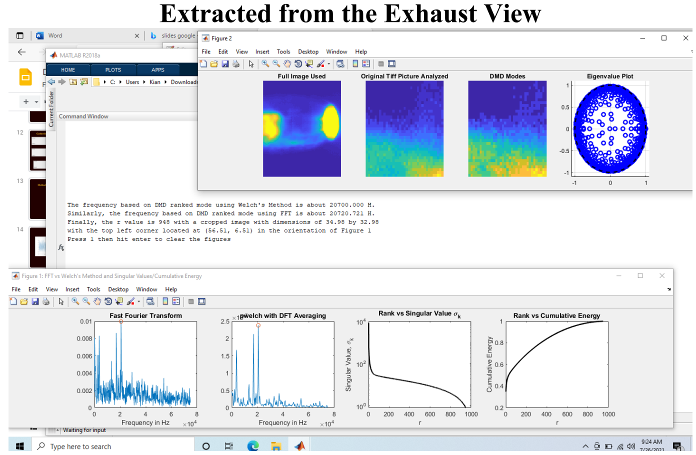


**Figure 18: Second Set of Detonation Wave Frequencies Extracted from the Exhaust View**

Figures 17 and 18 look at the exhaust views from Figures 13 and 14 respectively. As mentioned before, these tiff files had to be cropped to decrease the noise in the frequency domains. Furthermore, the frequency analysis is directly dependent on where the crop occurs because where the detonation waves can be detected is location specific. Figure 17's crop location was fairly straightforward to find because, even though the detonation waves cannot be directly seen, the paths left by these waves are still visible. Figure 18 on the other hand had a trickier approach as there was no sign of the detonation wave. This made the exhaust view in Figure 14 much harder to extract and, in Figure 18's graphs for frequency analysis (*Fast Fourier Transform* and *pwelch with DFT Averaging*), there are two main peaks at around 17 kHz and 20 kHz while Figure 17's graphs for frequency analysis show a peak at around 16.5 kHz. Also, one can easily see that, compared to Figures 15 and 16, Figures 17 and 18 show frequency domains with more noise interference (most likely because of the view covering more area because of how the views differed from Figures 15 and 16. Finally, all of the frequency analyses except for the one done in Figure 18 have had peaks that corresponded relatively close to the actual operational frequencies of the RDEs that were operated on.

 

Plus, with the cropped part of Figure 14 used for Figure 18's graph demonstration, this cropped image was specifically picked after multiple attempts to find a cropped image that would get a similar result. Furthermore, the two peaks were difficult to isolate into one peak and doing so would consume more time than is needed because the cropping for this exhaust view is highly specific.

## CONCLUSION/FURTHER WORK

DMD has been demonstrated to find frequencies of detonation waves produced inside RDE's and worked relatively well. It was only at the last exhaust view (Figures 14 and 18) that there were issues and that was in the case of having two peaks from the cropped view rather than just one peak.

Moving forward, this DMD analysis of detonation waves would lead to attaching a nozzle to the back-end of the RDE and see if the frequency at the back-end reduces as a result of said nozzle.

## ACKNOWLEDGEMENTS

The National Department of Defense funded the REU HYPER Program at the University of Central Florida, administered by Dr. Kauffman and Dr. Gordon. Special thanks to PhD. Students Robert Burke and Taha Rezzag for the mentorship, Dr. Kareem Ahmed for administering the research, and fellow undergraduate student Julio Machado for helping with other parts of the research.

## REFERENCES

1. Lu F. K. and Braun E. M. "Rotating Detonation Wave Propulsion: Experimental Challenges, Modeling, and Engine Concepts," *JOURNAL OF PROPULSION AND POWER*. Vol. 30, No. 5, September–October 2014, pp. 1125-1139.
2. *Technology Development Status of Pressure Gain Combustion for Power Generating Gas Turbines:* EPRI, Palo Alto, CA: 2019. 3002015798.
3. Turns, S. R. *An Introduction to Combustion: Concepts and Applications*: McGraw-Hill, 2012.
4. Bennewitz, J. W., Bigler, B. R., Hargus, W. A., Danczyk, S. A., and Smith, R. D. "Characterization of detonation wave propagation in a rotating detonation rocket engine using direct high-speed imaging," *2018 Joint Propulsion Conference*. 2018.
5. Brunton B. W., Brunton S. L, Kutz J. N.,and Proctor J. L. *Dynamic Mode Decomposition*: Society for Industrial and Applied Mathematics, 2016.
6. Brunton S. L, Kutz J. N., *Data-Driven Science and Engineering Machine Learning, Dynamical Systems, and Control*: Cambridge University Press, 2019.
7. Bohon. M. D., Orchini A., Bluemner R., Pashereit C. O., Gutmark E. J. "Dynamic mode decomposition analysis of rotating detonation waves," Springer Link, 3 November 2020.
8. Rezzag, T. (2020) Black_PERL_4_1_test.m (Version 4.1) [Source Code]
9. Higham J. (2019, January 18) POD_DMD.m (Version 1.2.0.1) [Source Code] https://www.mathworks.com/matlabcentral/fileexchange/65859-pod_dmd
10. Brunton S. [Steve Brunton] (2018, June 12). *Dynamic Mode Decompsition (Code)*. [Video]. YouTube.
11. (2012) FFTofNoisySignalExample.mlx [Live Code] https://www.mathworks.com/help/matlab/ref/fft.html
12. Cohen M. [Mike X Cohen] (2019, December 20). *Welch's method for smooth spectral decomposition*. [Video]. YouTube. https://www.youtube.com/watch?v=YK1F0-3VvQI
13. Robertson N. (2019, January 13). *Use Matlab Function pwelch to Find Power Spectral Density – or Do It Yourself.* Use Matlab Function pwelch to Find Power Spectral Density – or Do It Yourself - Neil Robertson (dsprelated.com)

 